

High Performance of In-situ Annealed Partial Pressurized Pulsed Laser Deposited (PLD) WO₃ & V₂O₅ Thin Film Electrodes for Flexible all Solid State Supercapbatteries

Ramasamy Velmurugan^{a,b}, Palaniappan Alagammai^a, Mani Ulaganathan^{a,b,*},
Balasubramanian Subramanian^{a,b,*}

^aCSIR- Central Electrochemical Research Institute, Karaikudi- 630 003, Tamil Nadu, India.

^bAcademy of Scientific and Innovative Research (AcSIR), (CSIR-HRDC) Campus,
Ghaziabad, Uttar Pradesh- 201 002, India.

Experimental Section:

All the films were prepared using PLD process; the experimental conditions used for the thin film preparation are listed in Table S1.

Table S1: Experimental parameters of PLD

Experimental parameter	value
Wavelength of KrF Eximer	248 nm
Laser Eximer Energy	400 mJ
Pulse replate rate	5 Hz
Pulse duration	10 ns
Target dimensions	2 inches × 5 mm
Chamber pressure	2×10^{-6} Torr
Film thickness	1 to 1.5 μ m
Deposition temperature	RT-650 °C

Capacitance Calculations:

The Areal capacitances of the three electrodes configuration was estimated from CV and GCD curves, respectively

$$C_S(\text{Areal}) = \frac{\oint i dV}{2A\vartheta\Delta V} \left(\frac{F}{\text{cm}^2} \right) \quad \text{-----} \quad (1)$$

Here $\vartheta \rightarrow$ Scan Rate, $A \rightarrow$ active area of the electrode, ΔV – Potential window

$\oint i dV$ – Area under the CV curve,

$$C_{DS}(\text{Areal}) = \frac{J_p \Delta t}{\Delta V} \left(\frac{F}{\text{cm}^2} \right) \quad \text{-----} \quad (2)$$

Here $J_p \rightarrow \frac{i}{A}$ Current density $\left(\frac{A}{\text{cm}^2} \right)$

The Volumetric capacitances was calculated from CV and GCD curves along with the following equation

$$C_{Vol} = \frac{\oint i dV}{2V_{vol} \vartheta \Delta V} \left(\frac{F}{\text{cm}^3} \right) \quad \text{-----} \quad (3)$$

$V_{total} =$ Volume of the device

$$C_{Vol} = \frac{J_p \Delta t}{\Delta V} \left(\frac{F}{\text{cm}^3} \right) \quad \text{-----} \quad (4)$$

$J_p \rightarrow \frac{i}{V_{vol}}$ Current density $\left(\frac{A}{\text{cm}^3} \right)$

The specific area and volumetric capacitance of the symmetric devices were calculated from CV and GCD curves by using following equation

$$C_{spec} = 2C_S \quad \text{-----} \quad (5)$$

The specific area and volumetric capacitances of the HSC device were investigated from GCD curves by using following relation

$$C_{spec} = 4C_S \quad \text{-----} \quad (6)$$

To construct an HSC, the charges stored on the electrodes are balanced using the below relation, The calculated specific capacitances (C) of single electrode, the voltage range for the HSC device by using GCD method (ΔV), and the active mass of the thin film electrodes (m), succeeding the equation:

$$\frac{m_+}{m_-} = \frac{C_{S-}\Delta V}{C_{S+}\Delta V} \quad \text{-----} \quad (7)$$

m_+ mass of the positive electrode, m_- mass of the negative electrodes; C_{S-} specific capacitance of the negative electrode and C_{S+} specific capacitance of the positive electrode obtained from the three electrode testing's.

The coulombic efficiency of the each GCD curve were calculated following the equation

$$\eta(\%) = \frac{\Delta t_d}{\Delta t_c} \times 100 \quad \text{-----} \quad (8)$$

Here $\Delta t_d \rightarrow$ discharging time, $\Delta t_c \rightarrow$ charging time

The volumetric specific energy density (E) and volumetric specific power density (P) alongside symmetric and HSC devices were estimated with the following equations

$$E = \frac{C_{cell}V^2}{3600} \quad \left(\frac{mWh}{cm^3}\right) \quad \text{-----} \quad (9)$$

$$P = \frac{E}{\Delta t_d} \times 3600 \quad \left(\frac{mW}{cm^3}\right) \quad \text{-----} \quad (10)$$

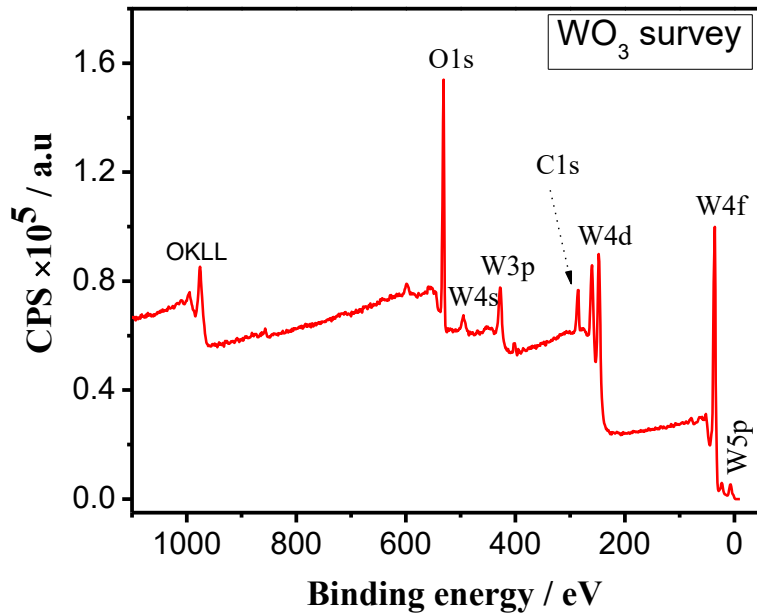


Figure S1: (a) XPS survey spectra of WO₃ thin film.

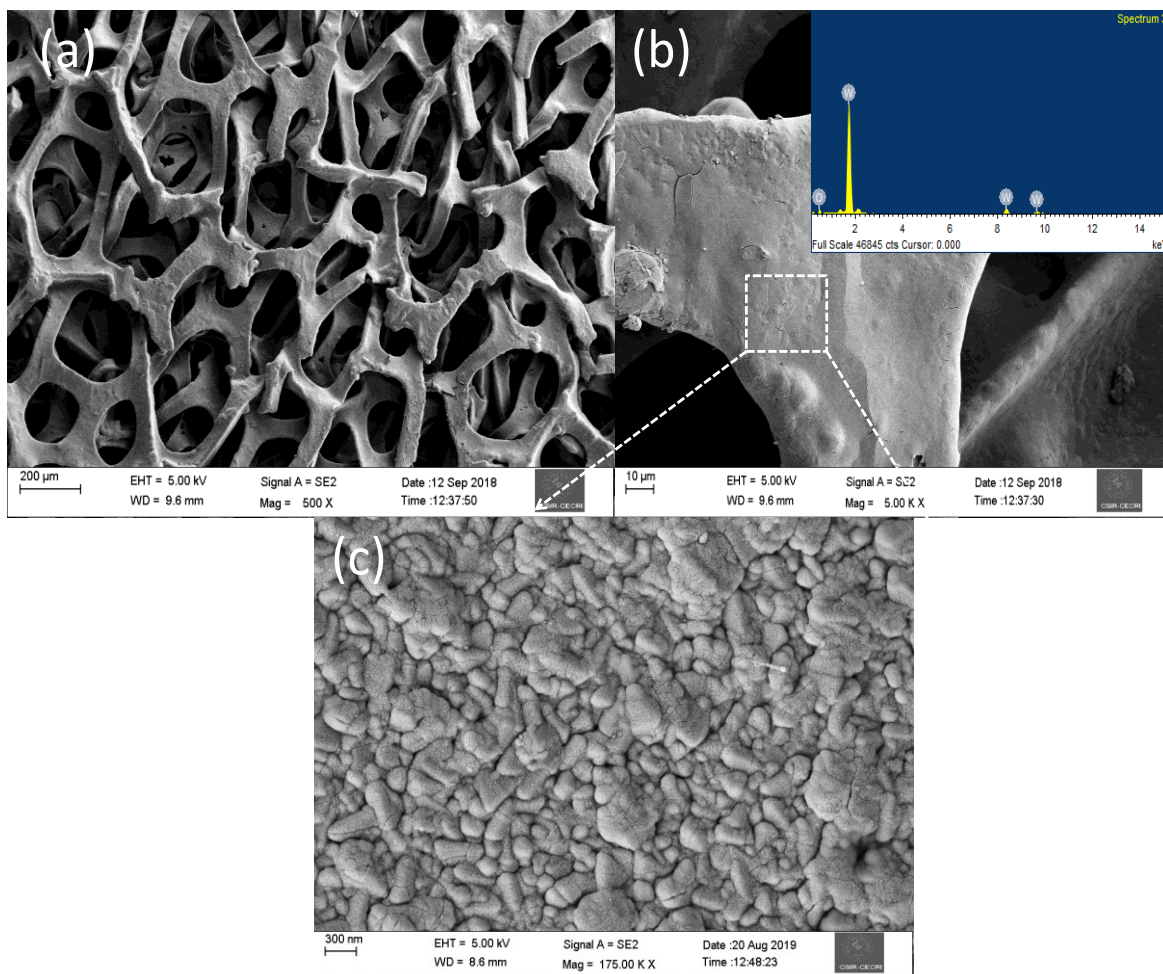


Figure S2: FESEM image of WO_3 annealed sample at different magnification coated on Ni-foam substrate: a) x 500; b) X 5k (inset view –EDAX spectrum) ; c) X 175k.

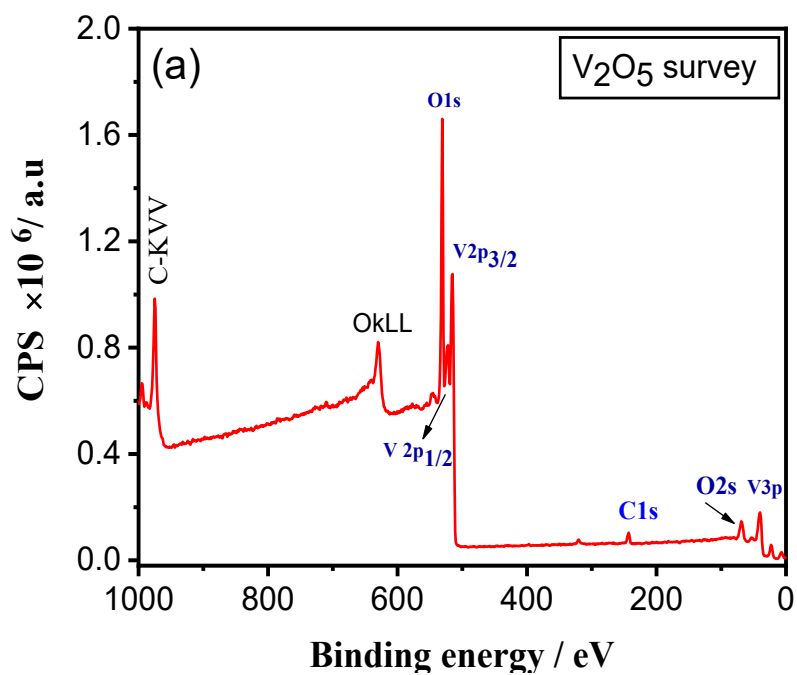


Figure S3: (a) XPS survey spectra of V_2O_5 thin film

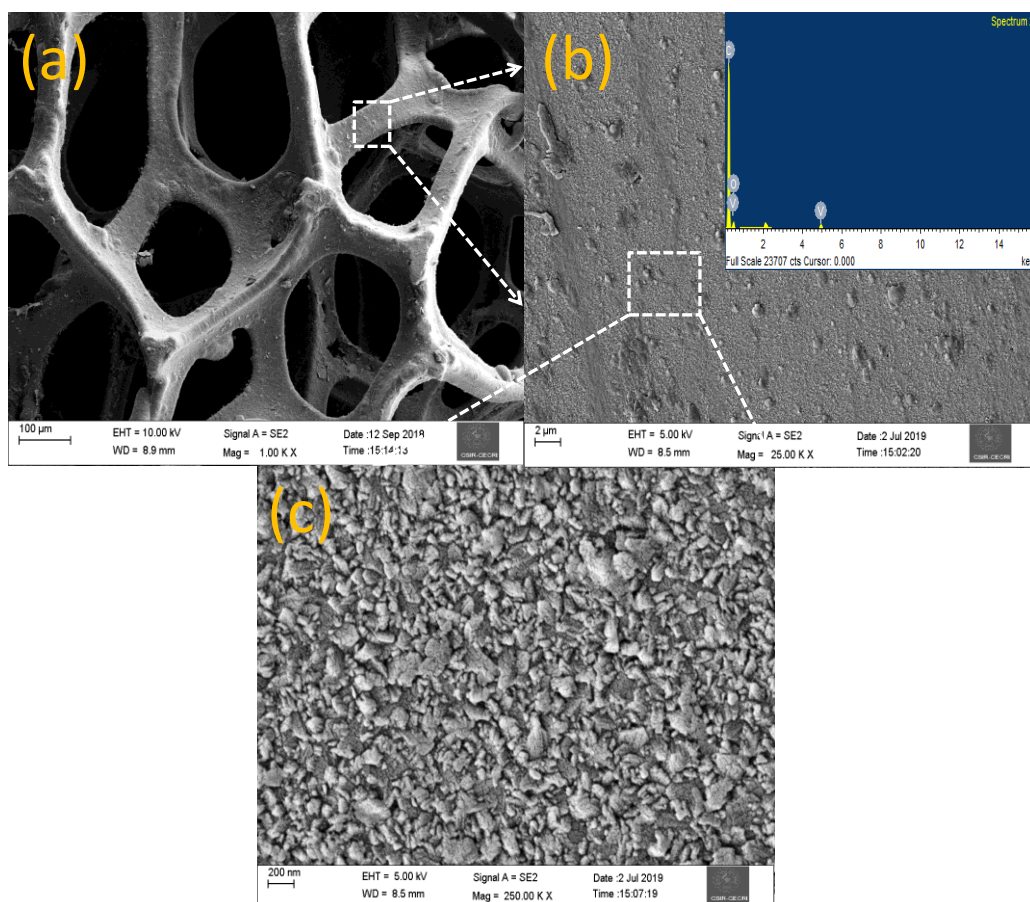


Figure S4: FESEM image of V_2O_5 annealed sample at different magnification coated on Ni-foam substrate: a) x 500; b) X 5k (inset view –EDAX spectrum) ; c) X 175k.

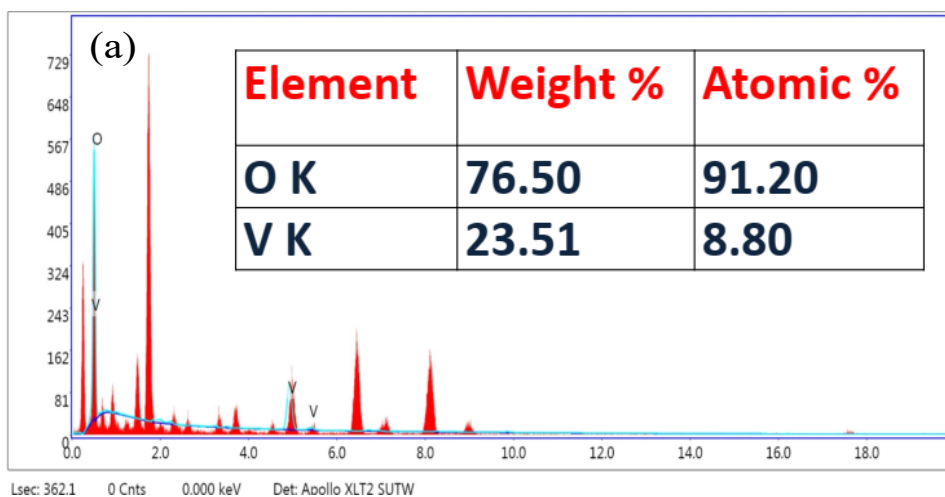


Figure S5; TEM EDAX spectrum of V_2O_5 thin film as prepared

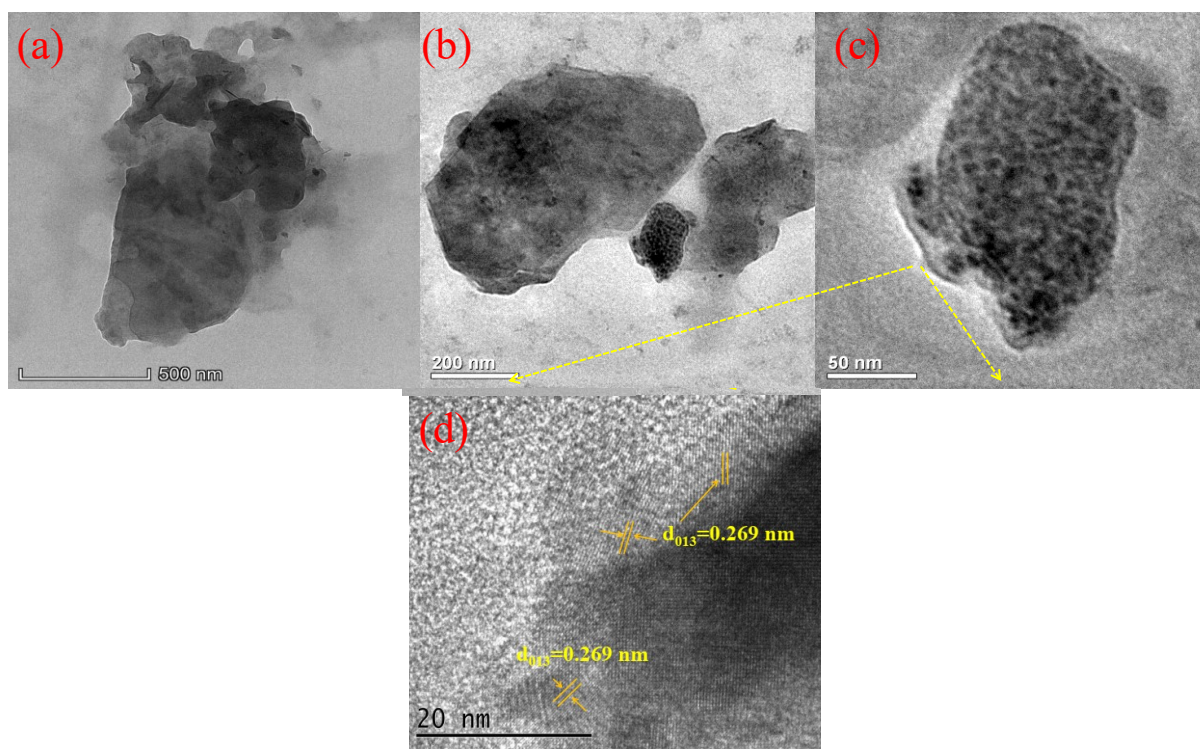


Figure S6: V_2O_5 thin film as prepared sample; (a-c) TEM images of the low and high magnifications; d) HR-TEM images with lattice planes;

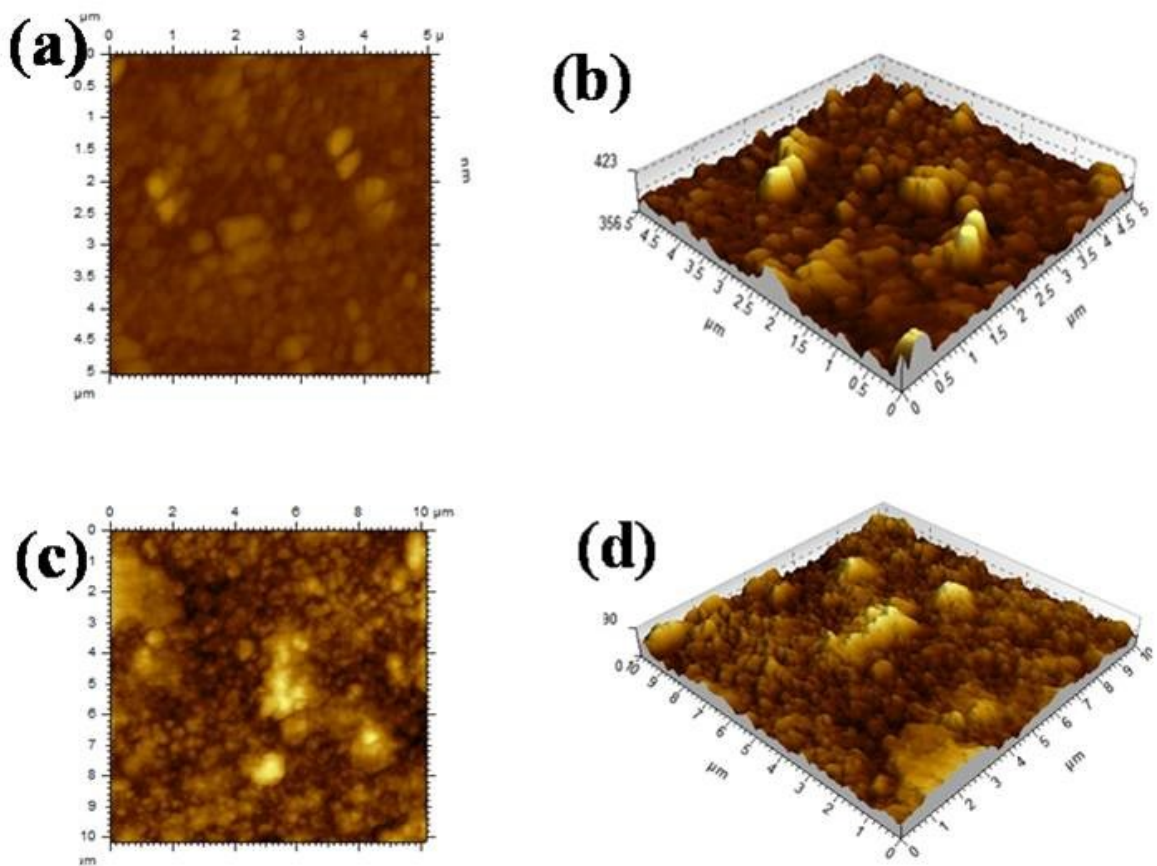


Figure S7; a-b) AFM 2D and 3D topographic images of V_2O_5 thin film; (c-d) AFM 2D and 3D topographic images of WO_3 thin film;

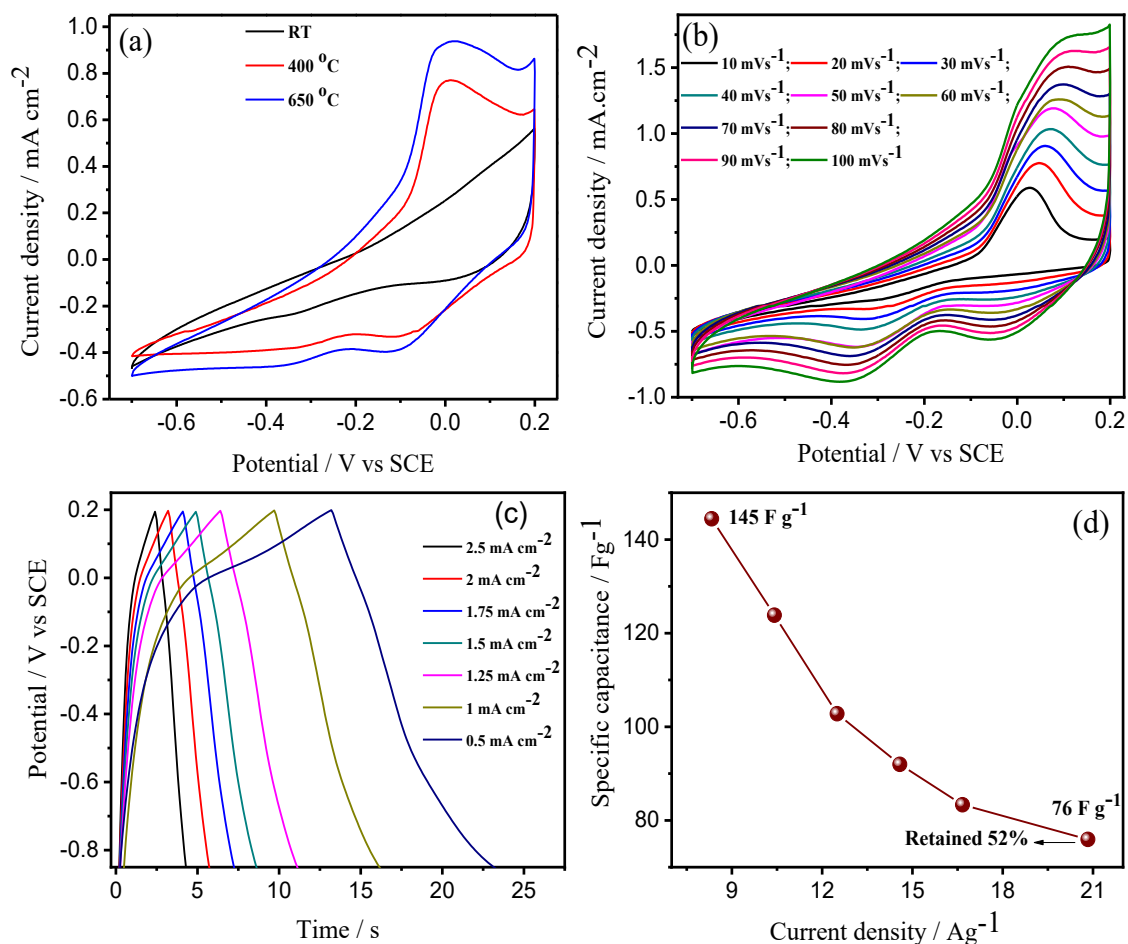


Figure S8; a) CV curve comparisons of the different WO₃ thin film electrodes annealed at different temperature in a three electrode configuration at scan rate of 50 mV. s⁻¹. ; (b) CV curves of the WO₃ thin film electrode different scan rates annealed at 650 °C tested at three electrode systems; (c) GCD profile curves of the sample annealed at 650 °C at different current density tested at three electrode systems; (d) Discharge capacitance vs. current density.

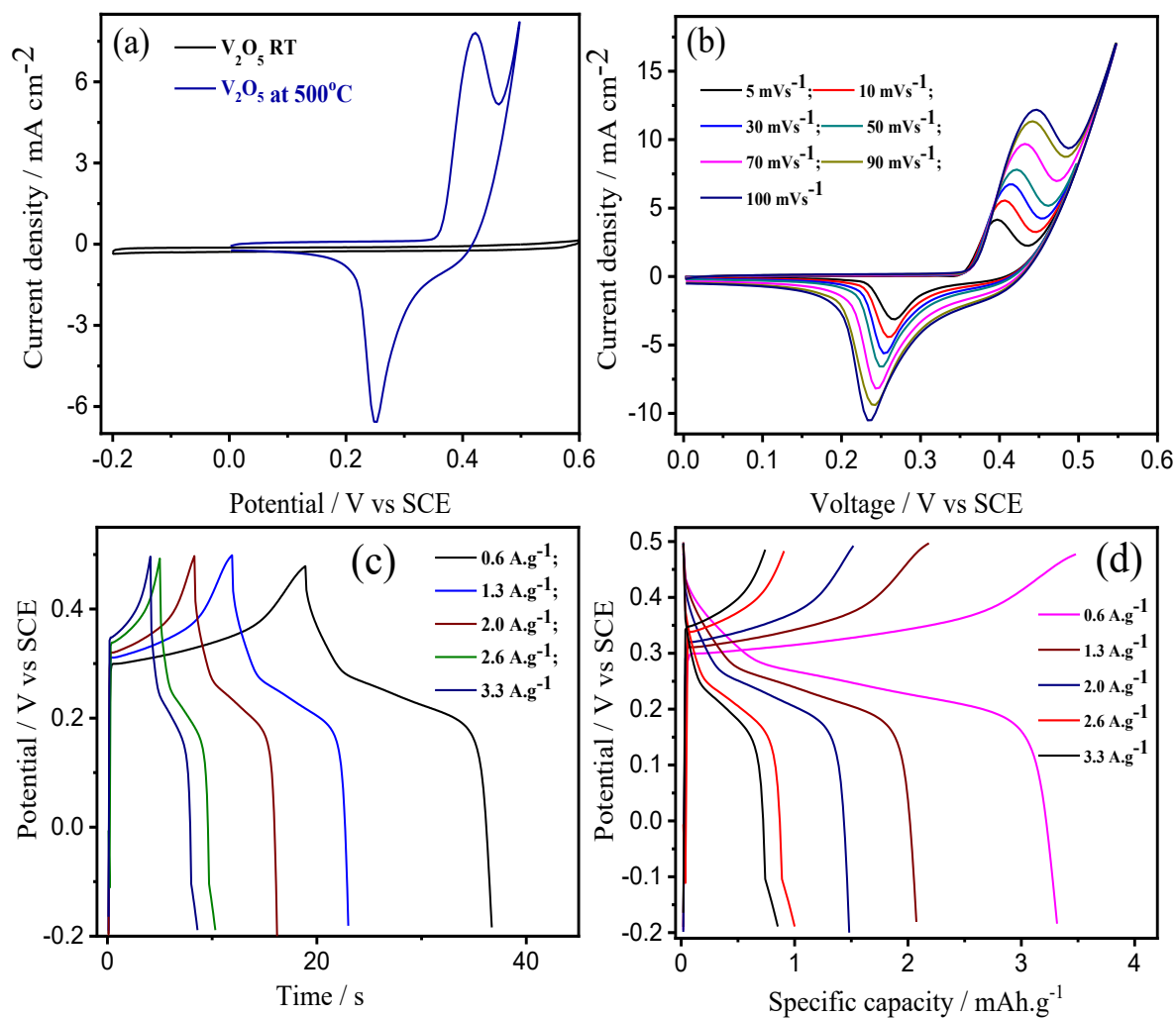


Figure S9: a) CV curve of as prepared and annealed at 500°C V_2O_5 coated carbon paper in a three electrode configuration at scan rate of 100 mV.s^{-1} ; (b) CV curves of the V_2O_5 thin film electrode different scan rates annealed at 500°C tested in a three electrode systems; (c) GCD curves of the sample annealed at 500°C at different current density tested at three electrode systems; (d) Specific capacity vs potential of the sample annealed at 500°C

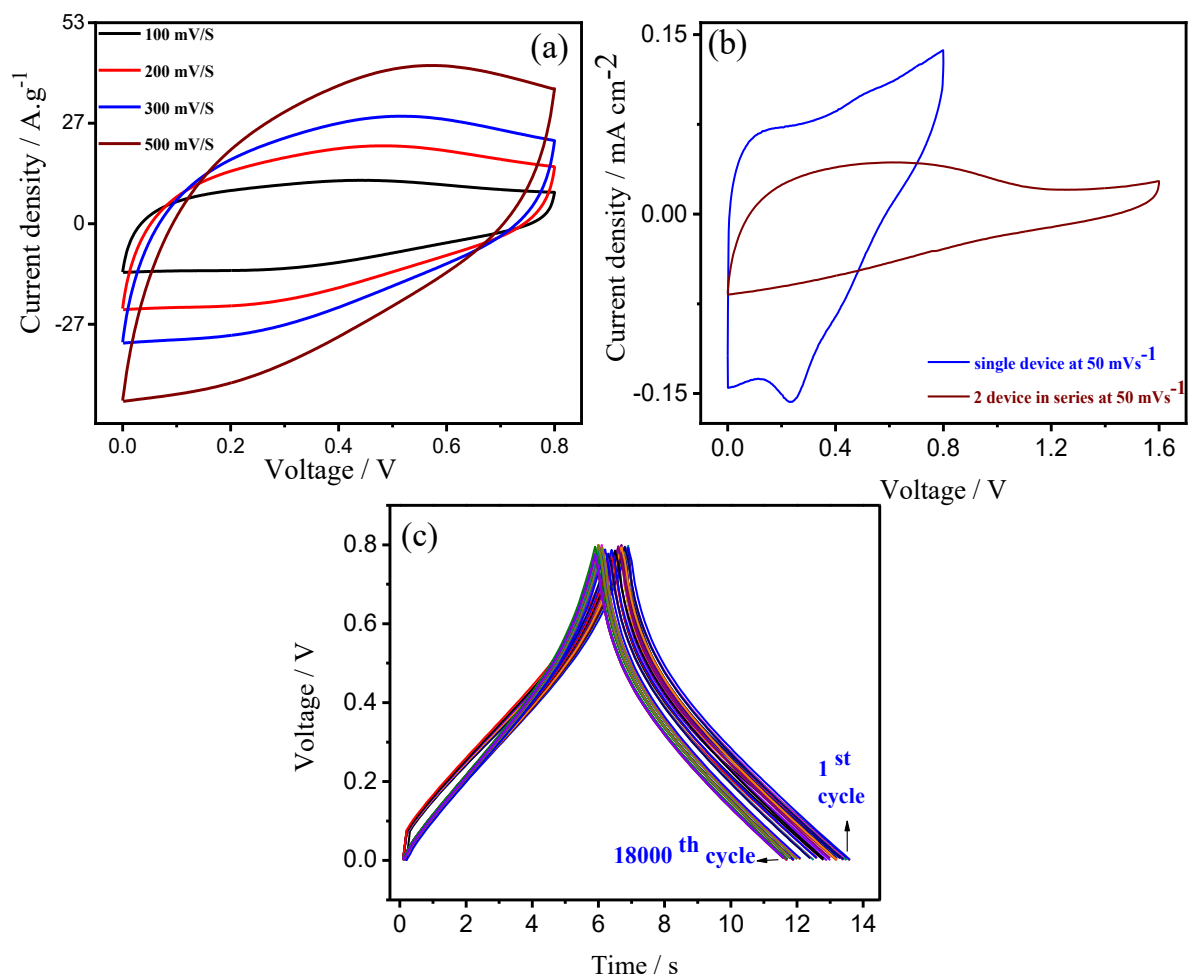


Figure S10; (a)CV curves performance of the WO_3 symmetric device at high scan rates ;(b) CV curves of WO_3 symmetric two devices in series; (c) GDC profile of WO_3 symmetric device stability curve for every 500th cycle up to 18k are compared.

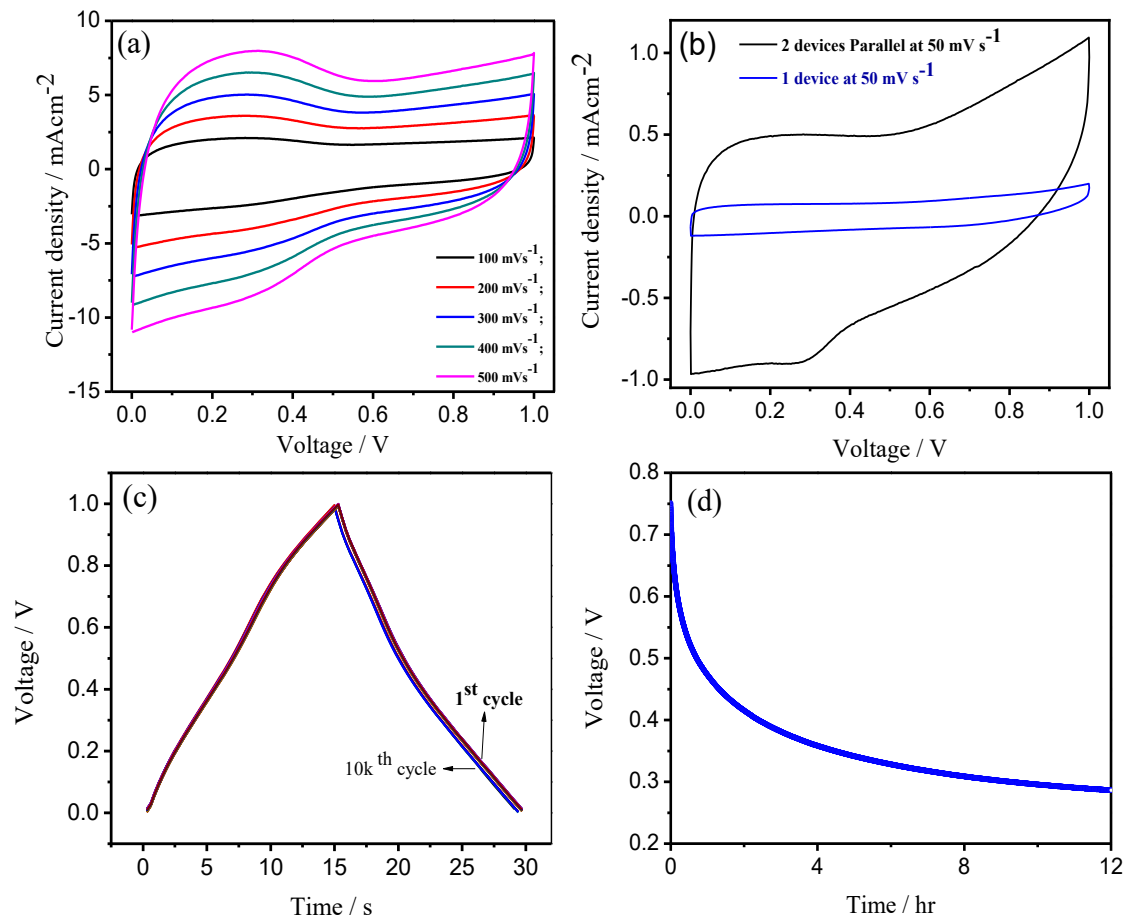


Figure S11 : (a) CV curves performance of the V_2O_5 symmetric device at high scan rates ;(b) CV curves of two devices in parallel at scan rate 50 mVs^{-1} ;(c) GCD profile comparisons of the V_2O_5 symmetric device stability every 1k cycles; (d) Self-discharge study of the V_2O_5 symmetric supercapacitor.

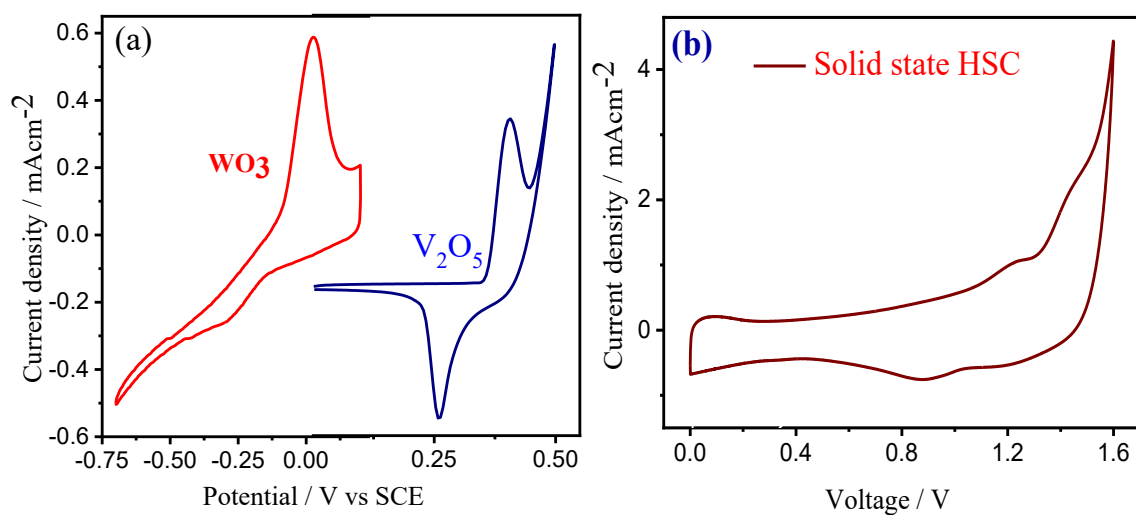


Figure S12; a) CV curve combination of positive and negative electrodes in a three electrode configurations at scan rate of $50 \text{ mV}\cdot\text{s}^{-1}$; b) CV curve of HSC device at scan rate of $50 \text{ mV}\cdot\text{s}^{-1}$.

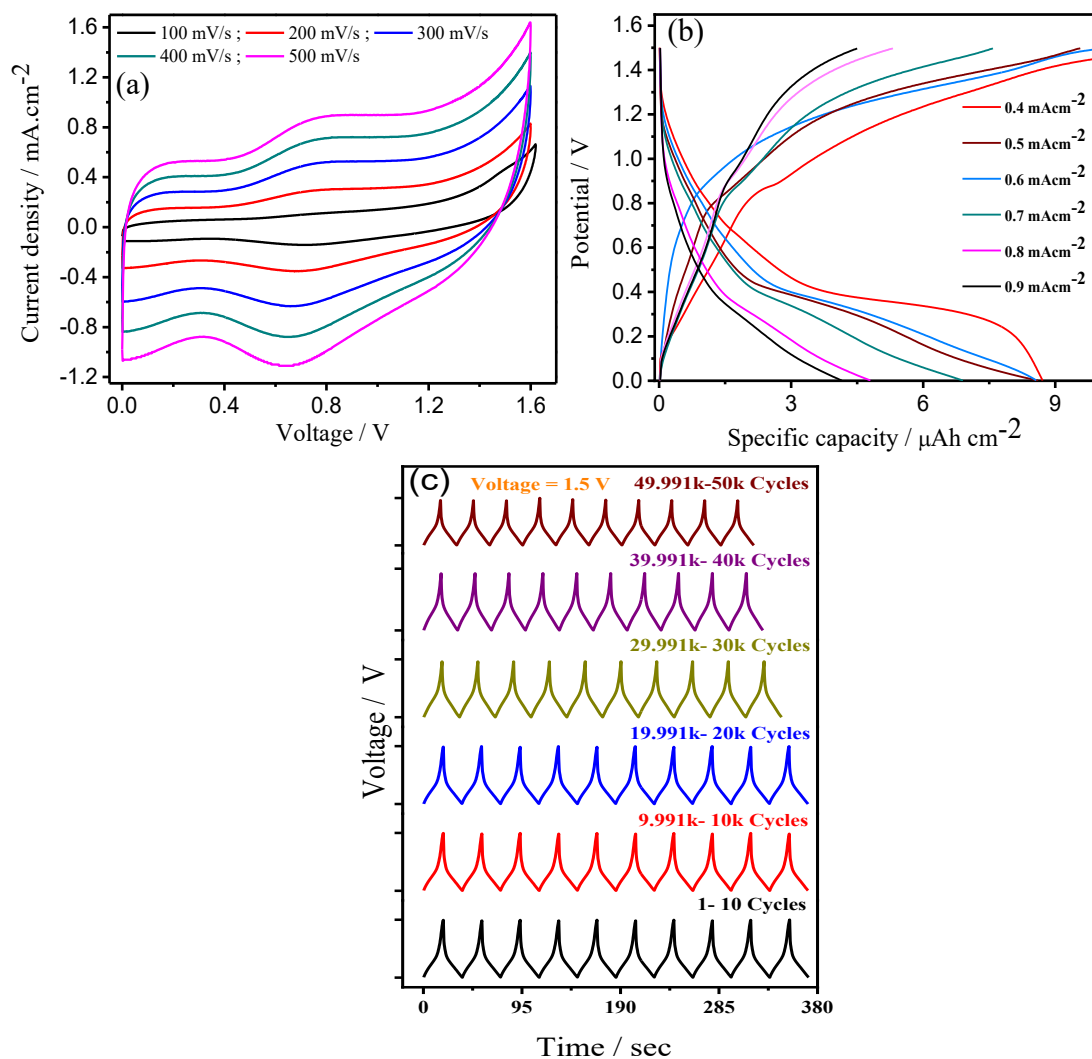


Figure S13; a) CV curves of solid state HSC device at high scan rates; (b) specific capacity curve at different current density; (c) GCD profile comparison of an HSC device at different cycle range.

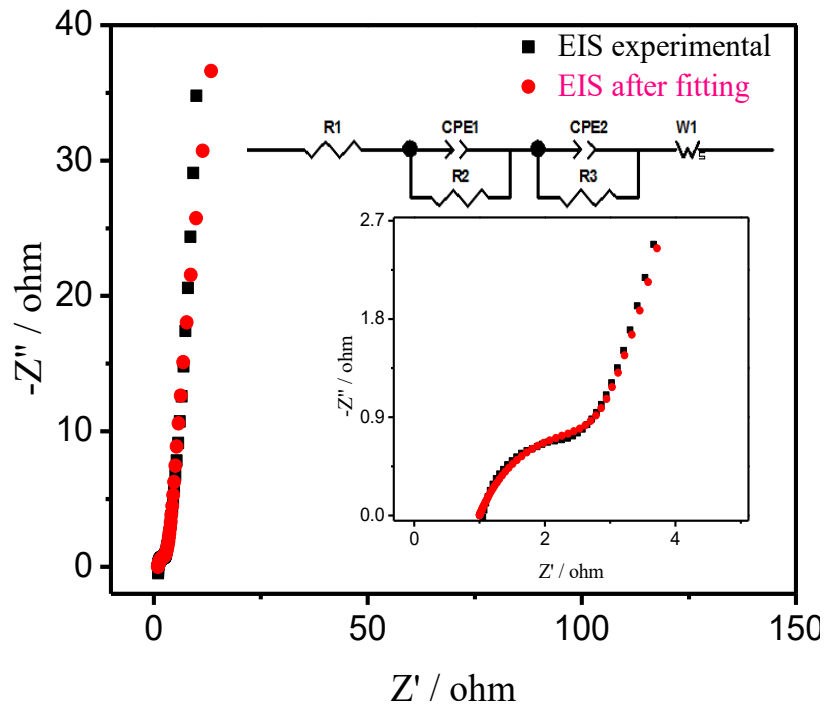


Figure S14; EIS analysis comparisons of the pristine solid state HSC device and after fitting EIS curve with equivalent circuit.

Table S2: EIS model fitting parameters

Element	Value	Error	Error%
R1	1	N/A	N/A
CPE1-T	0.21	N/A	N/A
CPE1-P	0.88	N/A	N/A
CPE2-T	0.03	N/A	N/A
CPE2-P	0.63	N/A	N/A
W1-R	0.627	N/A	N/A
W1-T	0.7	N/A	N/A
W1-P	0.5	N/A	N/A

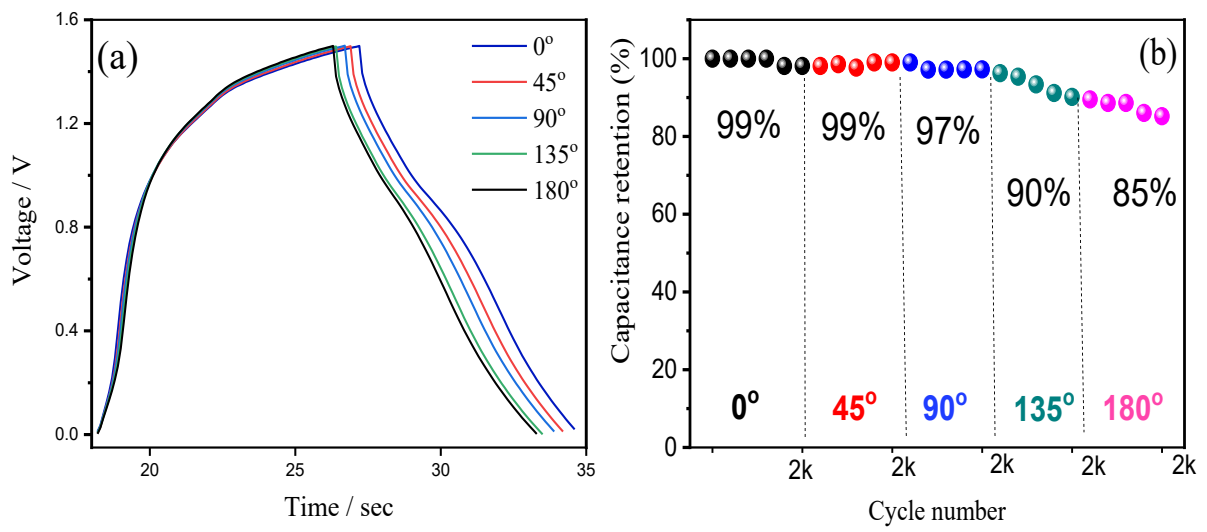


Figure S15; (a) GCD characteristics of solid state HSC device in various bending positions such as 0 to 180 deg; (b) capacitance retention curve at different bending angles such as 0 to 180 deg.

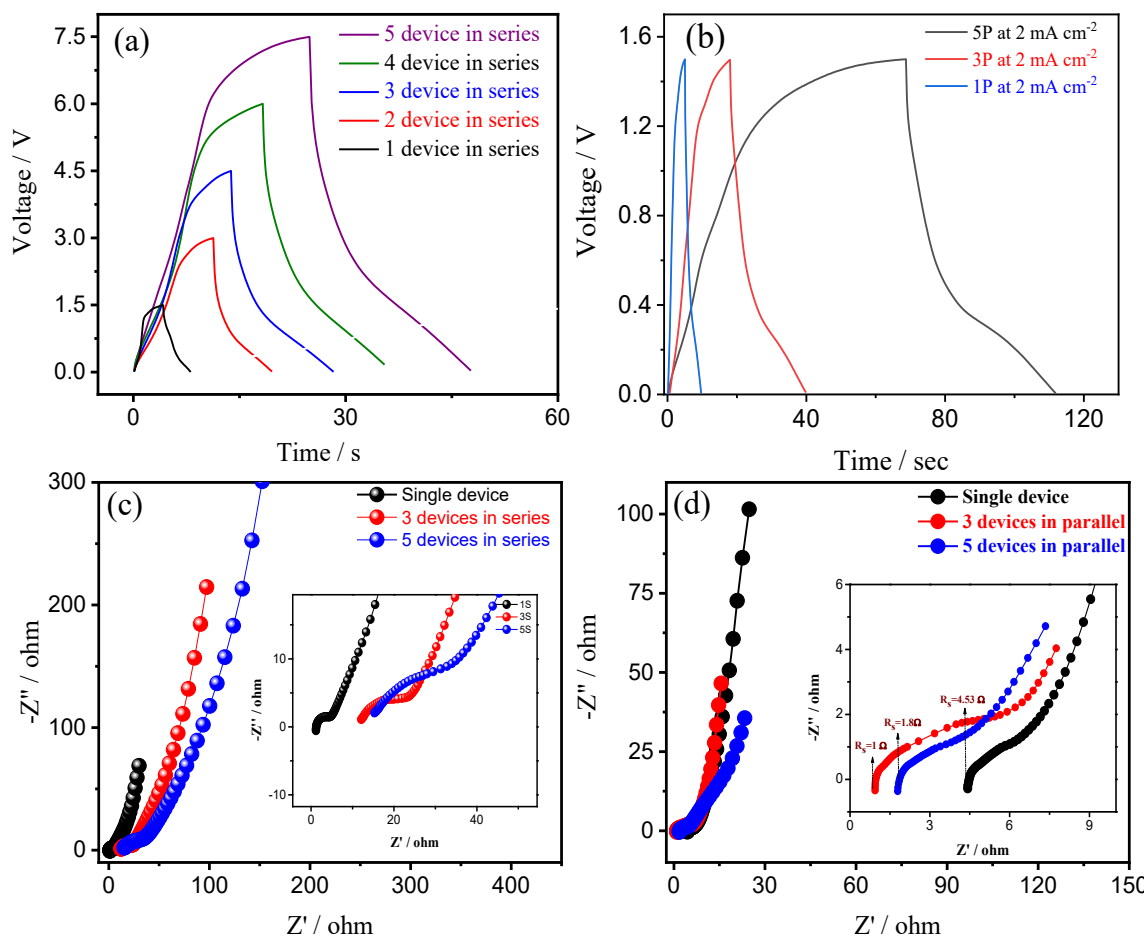


Figure S16; (a)GCD profile comparison solid state HSC devices in series combination at a current density of 5 mA.cm⁻²; (b)GCD profile comparison solid state HSC devices in parallel combination at a current density of 2 mA.cm⁻²; (c) EIS comparison solid state HSC devices in series combination; (d) EIS comparison solid state HSC devices in parallel combination.

Table S3: The electrochemical stability of the WO₃ thin film based supercapacitor comparison study with the reported literature

Reported Materials	Method	Electrolyte	Voltage Window [V]	Specific capacitance	Ref
WO ₃	SILAR	1 M Na ₂ SO ₄	0.8V	266 F g ⁻¹	[1]
WO ₃	Wet chemical method	1 M H ₂ SO ₄	-0.2 to -0.7	246 F g ⁻¹	[2]
WO ₃ Polymorphs	Hydrothermal	1M H ₂ SO ₄	-0.6 to 0.2V	377.5 F g ⁻¹	[3]
WO ₃	RF Magnetron sputtering	1M LiClO ₄ + PC	-0.9 and 0.5 V	228 F g ⁻¹	[4]
Pd-WO ₃	Hydrothermal	1M Na ₂ SO ₄	-0.7 to 0.1V	33.3 F g ⁻¹	[5]
WO ₃	Electrodeposition	1M H ₂ SO ₄	-0.5 to 0.2 V	138.2 F g ⁻¹	[6]
WO ₃ @W ₁₈ O ₄₉ -CNF	Electro-spinning	4 M KOH	-0.85-0.05 V	333.92 F g ⁻¹	[7]
MWCNTs-WO ₃	ZnNPs	1M H ₂ SO ₄	2.0 V	103 F g ⁻¹	[8]
WO₃	PLD	2M KOH	-0.2 to 0.7V	145 F g⁻¹	This work

Table S4: The electrochemical stability of the V₂O₅ thin film based supercapacitor comparison study with the reported literature

Reported Material /Symmetric Devices	Method	Electrolyte	Potential Window [V]	Specific capacitance	Ref
V ₂ O ₅ /MWC NT	Hydrothermal Method	H ₂ SO ₄ -HNO ₃	-0.2 to 0.8 v	410 F g ⁻¹	[9]
V ₂ O ₅ /PPY	Slurry	5 M LiNO ₃	0 to 1 V	448 F g ⁻¹	[10]
V ₂ O ₅ /Graphene	Atomic Layer Deposition	1M Na ₂ SO ₄	0 to 1 V	189 F g ⁻¹	[11]
V ₂ O ₅	Thermal treatment	0.5 M K ₂ SO ₄	-0.1 to 0.8 V	417 F g ⁻¹	[12]
V ₂ O ₅	Hydrothermal reduction	1M LiClO ₄	-0.3 to 1.1V	405 F g ⁻¹	[13]
V ₂ O ₅	Spray pyrolysis	1M KCl	-1.35 to 0.05V	307.3 F g ⁻¹	[14]
V ₂ O ₅	Hydrothermal	1M Na ₂ SO ₄	0 to 0.8V	177 Fg ⁻¹	[15]
Graphene /V ₂ O ₅	Hydrothermal	1M Na ₂ SO ₄	0 to 0.6 V	457 Fg ⁻¹	[16]
V ₂ O ₅	Thermal evaporation	PVA-KOH	0 to 1V	10 Fg ⁻¹	[17]
V₂O₅	PLD	2MKOH	0 to 0.6 V	433 Fg⁻¹	This work

Table S5: State of art of the thin film based electrode materials and their performance characteristics with other metal oxide symmetric supercapacitor

Reported SC Devices	Method	Electrolyte	Potential Window [V]	Specific Capacitance	Energy Density [Wh/ kg]	Power Density [kW/ kg]	Stability [Cycles]	Retention	Ref
MnO ₂	Pulsed Electrochemical Deposition	BMIBF ₄	1V	39.68 mF/ cm ²	---	----	--	---	[18]
α-MoO ₃	Hydrothermal	1 M H ₂ SO ₄	0.26–0.43 V	64 μF/ cm ²	---	----	720	----	[19]
MoO ₂	Magnetron Sputtering	0.5 M Li ₂ SO ₄	-0.8 to 0.2V	31 mF/ cm ²	----	---	12000	89%	[20]
(Fe,Cr) ₂ O ₃	Thermal Oxidization	2 M KOH	0 to -1 V	45.92 mF/cm ²	0.57 mWh/ cm ²	200 mW/ cm ²	10000	90%	[21]
NiCo ₂ O ₄ Symmetric	Electrospinning	PVA-KOH	1 V	42.6 mF/cm ²	----	----	5000	100%	[22]
MnO ₂	Electrodeposition	1.0 M Na ₂ SO ₄	0.8 V	52.55 mF/ cm ²	----	----	5000	90%	[23]
NiCo ₂ O ₄	Sol–Gel	2MKOH	-0.2 to 0.5 V	40.6 mF/cm ²	---	---	10,000	(96.5%)	[24]
TiO ₂	Atomic Layer Deposition	PVA/ H ₃ PO ₄	0.8 V	8.6 mF/cm ²	----	---	5000	95%	[25]
WO₃	PLD	PVA-KOH	0 to -0.8V	5.31mF/cm² 49.4 F/cm³	1.87 mWh/ cm³	0.54 W/ cm³	18000	88.8 %	This work
V₂O₅	PLD	PVA-KOH	0 to 1.0V	6.5 mF/cm² 44.21 F/cm³	1.71 mWh/ cm³	0.68 W/ cm³	10000	90.2 %	This work

Table S6: HSC device comparative study of electrochemical performance of volumetric capacitance with the reported literature.

Reported ASC Devices	Potential Window [V]	Volumetric Capacitance	Energy Density	Power Density	Stability [Cycles]	Retention	Ref
α -MnO ₂ NW/ Fe ₂ O ₃ NT	1.6V	1.5F cm ⁻³	0.55 mW h cm ⁻³	139.1 mW/cm ³	6000	90%	[26]
CNT-WO ₃	1.4 V	2.6 F cm ⁻³	0.59 mW h cm ⁻³	30.6 mW/cm ³	50 000	75.8%	[27]
V ₂ O ₅ /MWCNT	1.8 V	31 F cm ⁻³	2.1mW h cm ⁻³	1.5 W/cm ³	5000	100%	[28]
α -Fe ₂ O ₃ /MnO _x NR	1 V	1.28 F cm ⁻³	0.64 mW h cm ⁻³	155 mW/cm ³	4000	78%	[29]
Co ₉ S ₈ NR// RuO ₂ NS	1.6 V	4.3 F cm ⁻³	1.21 mW h cm ⁻³	13.29 W/cm ³	2000	90%	[30]
NiCo ₂ O ₄ NS	1V	10.3 F cm ⁻³	1.44 mW h cm ⁻³	17W/cm ³	500	92%	[31]
RuO ₂ -WO ₃	1.6 V	3.52 F cm ⁻³	1.25 mW h cm ⁻³	40 mW/cm ³	6500	100%	[32]
WO ₃ /MnO ₂	1.8 V	7.22 F cm ⁻³	3.25 mW h cm ⁻³	411 mW/cm ³	6000	89%	[33]
Fe ₂ O ₃ /MnO ₂	1.2 V	60 F·cm ⁻³	12 mWh cm ⁻³	14.8 Wcm ⁻³	2,500	80%	[34]
WO ₃ / G/PT	1.6	167.6 mF cm ⁻³	60 μ Wh cm ⁻³	2320 μ Wcm ⁻³	3000	99%	[35]
rGO/H-Fe ₂ O ₃	1.5	37.88 mF cm ⁻²	0.14 mW h cm ⁻³	12.30 W cm ⁻³	10 000	97%	[36]
WO₃-V₂O₅	1.5 V	40.28 Fcm⁻³	12.6 mW h cm⁻³	1.42 W cm⁻³	50000	95%	This work

References:

- [1]. VaibhavLokhande, AbhishekLokhande, GonNamkoong , Jin HyeokKim, TaeksooJi, Chargestoragein; *Results in Physics* 12 (2019) 2012–2020
- [2]. P. Periasamy, T. Krishnakumar, M. Sathish,Murthy Chavali, Prem Felix Siril, V. P. Devarajan; *Materials in Electronics* (2018) 29:6157–6166
- [3]. AkbarI. Inamdar, Jongmin Kim, Yongcheol Jo, Hyeonseok Woo, Sangeun Cho, Sambhaji M.Pawar, Hyungsang Kim,Hyunsi kIm; *Solar Energy Materials & Solar Cells* 166 (2017) 78–85
- [4]. ShobhnathP.Gupta, VandanaB.PatilNilesh, L.Tarwal, ShekharD.Bhame, SureshW.Gosavi ,ImtiazS.Mulla , DattatrayJ.Late , SharadS.Suryavanshi ,PravinS.Walke ; *Materials Chemistry and Physics* 225 (2019) 192–199
- [5]. Shobhnath P.Gupta,Vandana B.Patil Nilesh, L.Tarwal, Shekhar D.Bhame,Suresh W.Gosavi ,Imtiaz S.Mulla ,Dattatray J.Late , Sharad S.Suryavanshi ,Pravin S.Walke *Materials Chemistry and Physics* 225 (2019) 192–199
- [6]. Liuxue Shen, Lianhuan Du, Shaozao Tan, ZhigangZang, Chuanxi Zhao, and Wenjie Mai ; *Chem. Commun.*,2016, 52, 6296
- [7]. Masoud Faraji, Roya Khalilzadeh Soltanahmadi, Hossein Mohammadzadeh Aydisheh Borhan Mostafavi Bavan ; *Ionics* 26, 2021–2029(2020)
- [8]. Masoud Faraji, Roya Khalilzadeh Soltanahmadi, Hossein Mohammadzadeh Aydisheh Borhan Mostafavi Bavan *Ionics* 26, 3003–3013(2020)
- [9]. Balakrishnan Saravanakumar, Kamatchi Kamaraj Purushothaman and Gopalan Muralidharan ; *RSC Adv.*, 2014, 4, 37437
- [10]. Tao Qian, Na Xu, JinqiuZhou,Tingzhou Yang, Xuejun Liu, XiaoweiShen, Jiaqi Liangand Chenglin Yan; *J. Mater. Chem. A*, 2015, 3,488
- [11]. Seung-Mo Lee, Yong-Jin Park, Do Van Lam, Jae-Hyun Kim, Kyubock Lee; *Applied Surface Science* 512 (2020) 145626

- [12]. R.B.Rakhi, D.H.Nagaraju, Pierre Beaujuge, H.N.Alshareef;, *ElectrochimicaActa*.electacta.2016.10.109
- [13]. Rahul S. Ingole, B.J. Lokhande; *J Mater Sci: Mater Electron* (2016) 27:1363–1369
- [14]. RamuManikandan, Chellan Justin Raj, Murugesan Rajesh, ByungChul Kim , Seungil Park ,Kook Hyun Yu; *Adv. Mater. Interfaces* 2018, 5, 1800041
- [15]. Tao Peng, Jun Wang, Qi Liu, Jingyuan Liu and Peng Wangl; *CrystEngComm* c4ce02305f
- [16]. Yaju Zhou, Linlin Sun, Dongyao Wu, Xin Li, Jinze Li, Pengwei Huo, Huiqin Wang, Yongsheng Yan; *Journal of Alloys and Compounds* 817, 2020, 152707
- [17]. RamasamyVelmurugan, JayaramanPremkumar, RagupathyPitchai, Mani Ulaganathan Balasubramanian Subramanian ; *Accsuschemeng*. 2019, 7, 15, 13115–13126
- [18]. AmrObeidat, Mohammad A. Gharaibeh; *INTERNATIONAL JOURNAL of RENEWABLE ENERGY RESEARCH*
- [19]. Beatriz Mendoza-Sánchez, ThierryBrousse, ClaudiaRamirez-Castro, ValeriaNicolosi, PatrickS. Grant; *ElectrochimicaActa* 91 (2013) 253– 26
- [20]. Can Liu, Zhengcao Li, and Zhengjun Zhang;; *Science and Technology of Advanced Materials, Sci. Technol. Adv. Mater.* 14 065005
- [21]. Prashant R. Deshmukh, YoungkuSohn, WeonGyu Shin; *ACS Sustainable Chem. Eng.* 2018, 6, 1, 300–310
- [22]. Yuanfei Ai, Jing Ma and Zhiming M Wang; *Earth and Environmental Science* 170 (2018) 032095
- [23]. Soomin Park, Inho Nam, Gil-Pyo Kim,Jeong Woo Han, JongheopYi; *ACS Appl. Mater. Interfaces* 2013, 5, 9908–9912
- [24]. Yang Liu, Ni Wang, Chengtao Yang, Wencheng Hu, *Ceramics International*42(2016)11411–11416
- [25]. Kuan Hu, Chao Zheng, Miao An, Xiaohui Ma and Lu Wang; *J. Mater. Chem. A*, 2018, 6, 8047–8052
- [26]. Peihua Yang, Yong Ding, Ziyin Lin, Zhongwei Chen, YuzhiLi, PengfeiQiang, MasoodEbrahimi, WenjieMai, Ching Ping Wong, Zhong Lin Wang; *Nano Lett* 2014, 14, 2, 731–736.

- [27]. Peng Sun, Zewei Deng, Peihua Yang, Xiang Yu, Yanli Chen, Zhimin Liang, HuiMeng, Weiguang Xie, Shaozao Tan and Wenjie Mai ; *J. Mater. Chem. A*, 2015, 3, 12076
- [28]. Li Hua, Zhongyuan Ma, Peipei Shi, Li Li, Kun Rui, Jinyuan Zhou, Xiao Huang, Xiang Liu, Jixin Zhu, Gengzhi Sun and Wei Huang; *J. Mater. Chem. A*, 2017, 5, 2483.
- [29]. Debasish Sarkar, Somnath Pal, Suman Mandal, Ashok Shukla, and D. D. Sarma; *Journal of The Electrochemical Society*, 164 (12) A2707-A2715
- [30]. Jing Xu, Qiufan Wang, Xiaowei Wang, Qingyi Xiang, Bo Liang, Di Chen, Guozhen Shen; *ACS Nano* 5453–5462
- [31]. Qiufan Wang, Xianfu Wang, Jing Xu, Xiaouyang, Xiaojuan Hou, Di Chen, Rongming Wang, Guozhen Shen; *j.nanoen*.2014.05.014
- [32]. Su - Hyeon Ji, Nilesh R. Chodankar, Do-Heyoung Kim; *Electrochimica Acta* 325 (2019) 134879
- [33]. Debasish Sarkar, Soham Mukherjee, Somnath Pal, D. D. Sarma and Ashok Shukla; *J. Electrochem. Soc.* **165** A2108.
- [34]. Zehua Liu, Xiaocong Tian, Xu Xu, Liang He, Mengyu Yan, Chunhua Han, Yan Li, Wei Yang, Liqiang Mai ; *Nano Research*, **10**, 2471–2481(2017)
- [35]. Li-Na Jin, Ping Liu, Chun Jin, Jia -Nan Zhang, Shao-Wei Bian; *Journal of Colloid and Interface Science*, 10, 15, 1-11
- [36]. Qiyong Lv, Kai Chi, Yan Zhang, Fei Xiao, Junwu Xiao, Shuai Wang and Kian Ping Loh ; *J. Mater. Chem. A*, 2017, 5, 2759–2767